

# Penetration of $\beta$ -Lactoglobulin into Monoglyceride Monolayers. Dynamics, Interactions, and Topography of Mixed Films

Marta Cejudo Fernández, Cecilio Carrera Sánchez, Rosario Rodríguez Niño, and Juan M. Rodríguez Patino\*

Departamento de Ingeniería Química, Facultad de Química, Universidad de Sevilla, C/. Prof. García González 1, 41012-Seville, Spain

Received: August 2, 2006; In Final Form: September 11, 2006

In this work we have analyzed the penetration of  $\beta$ -lactoglobulin into a monoglyceride monolayer (monopalmitin or monoolein) spread at the air–water interface and its effects on the structural, dilatational, and topographical characteristics of mixed films. Dynamic tensiometry, surface film balance, Brewster angle microscopy (BAM), and surface dilatational rheology have been used, maintaining the temperature constant at 20 °C and the pH and ionic strength at 7 and 0.05 M, respectively. The initial surface pressure (mN/m) of the spread monoglyceride monolayer ( $\pi_{\text{MONOGLYCERIDE}}$ ) at 10, 20, and the collapse point is the variable studied.  $\beta$ -Lactoglobulin can penetrate into a spread monoglyceride monolayer at every surface pressure. The penetration of  $\beta$ -lactoglobulin into the monoglyceride monolayer with a more condensed structure, at the collapse point of the monoglyceride, requires monoglyceride molecular loss by collapse and/or desorption. However, the structural, topographical, and dilatational characteristics of monoglyceride penetrated by  $\beta$ -lactoglobulin mixed monolayers are essentially dominated by the presence of monoglyceride (either monopalmitin or monoolein) in the mixed film. In fact, monoglyceride molecules have the capacity to re-enter the monolayer after expansion and recompression of the mixed monolayer. Thus, monoglyceride molecular loss by collapse and/or desorption is reversible. The topography of the monolayer under dynamic conditions corroborates these conclusions.

## Introduction

The way in which the constituent emulsifiers (lipids, phospholipids, proteins, etc.) adsorb and interact at fluid interfaces has an effect on the interfacial characteristics of adsorbed films,<sup>1</sup> which in turn affect the stability and mechanical properties of dispersed food systems (emulsions and foams). The optimum use of emulsifiers depends on knowledge of their interfacial physicochemical characteristics—such as surface activity, structure, miscibility, superficial viscosity, and so forth—and the kinetics of the film formation at fluid interfaces.<sup>2,3</sup> In addition, in many emulsifier applications, mixtures of different emulsifiers often exhibit properties superior to those of the individual emulsifier alone due to synergistic interactions between emulsifier molecules. In previous works with mono- and diglycerides<sup>4,5</sup> or mixtures of monoglycerides and milk proteins<sup>6</sup> we have observed that when molecules of both emulsifiers are spread at the air–water interface they are more expanded or packed more closely together than when either emulsifier is present alone, indicating some form of association. Interactions between molecules of emulsifiers could affect not only the film structure and topography but also dynamic phenomena in mixed films.<sup>6,7</sup>

In this contribution we are concerned with the analysis of dynamic, structural, topographical, and dilatational characteristics of mixed films formed by the penetration of  $\beta$ -lactoglobulin into monoglyceride monolayers (monopalmitin and monoolein) previously spread at the air–water interface. Information about the static and dynamic characteristics of adsorbed mixed films would be very helpful in the prediction of optimized formulations for food foams and emulsions. So far, there are

important experimental results available on structural characteristics of mixed emulsifiers spread at the air–water interface.<sup>6,8–10</sup> However, as far as we know, there have been few studies of the structural characteristics of adsorbed films at the air–water interface,<sup>7,11,12</sup> although in practice mixtures of these emulsifiers are usually used in order to achieve an optimal effect in food formulations.<sup>8,9</sup> These experiments mimic the behavior of mixed emulsifiers in most food emulsions in which an oil-soluble lipid (monopalmitin or monoolein) is adsorbed faster than a protein at the interface.<sup>1</sup> This leads to the formation of a lipid monolayer, into which the protein can subsequently penetrate, and this is followed by lipid–protein interactions.<sup>2,3</sup> Thus, for food dispersion formulations (emulsions and foams), the penetration of a protein into a lipid or phospholipid monolayer is of special interest. In fact, although spread monolayers have demonstrated their relevance for fundamental studies,<sup>4–6</sup> adsorbed or penetrated monolayers are more interesting from a technological point of view.<sup>7</sup> These results may have direct relevance for foam formation and stabilization and, assuming the validity of extrapolating from the air–water interface to the oil–water interface, also for emulsions.

## Experimental Section

**Chemicals.** Synthetic 1-monoheptadecanoyl-*rac*-glycerol (monopalmitin, DIMODAN PA 90) and 1-mono(*cis*-9-octadecanoyl) glycerol (monoolein, RYLO MG 19) were supplied by Danisco Ingredients (Brabran, Denmark) with over 95–98% of purity. Whey protein isolate (WPI), a native protein with very high content of  $\beta$ -lactoglobulin (protein 92  $\pm$  2%,  $\beta$ -lactoglobulin > 95%,  $\alpha$ -lactalbumin < 5%) obtained by fractionation, was supplied by Danisco Ingredients. Samples for protein solutions were prepared using Milli-Q ultrapure water

\* To whom all correspondence should be addressed. Tel.: +34 95 4556446. Fax: +34 95 4556447. E-mail: jmrodri@us.es.

and were buffered at pH 7. Monoglycerides were spread in the form of a solution, using hexane/ethanol (9:1, v/v) as a spreading solvent. Analytical grade hexane (Merck, 99%) and ethanol (Merck, >99.8%) were used. A commercial buffer solution called trizma ((CH<sub>2</sub>OH)<sub>3</sub>CNH<sub>2</sub>/(CH<sub>2</sub>OH)<sub>3</sub>CNH<sub>3</sub>Cl, Sigma, >99.5%) was used to achieve pH 7. Ionic strength was 0.05 M in all the experiments. Sodium azide (Sigma) was added (0.05 wt %) as an anti-microbial agent.

**Dynamic Surface Pressure Measurements.** The study of the dynamics of penetration of  $\beta$ -lactoglobulin into a monoglyceride monolayer spread at the air–water interface was performed on a fully automated Wilhelmy-type film balance, by following the time evolution of the surface pressure and film topography (morphology and reflectivity) after the injection of a  $\beta$ -lactoglobulin solution underneath the monoglyceride monolayer.<sup>1</sup> Before each measurement, the film balance was calibrated at 20 °C, as described previously.<sup>13,14</sup> The monoglyceride solutions in hexane/ethanol (9:1, v/v) were spread on the subphase by means of a micrometric syringe at 20 °C. Aliquots of 300–350  $\mu$ L (from  $1.5 \times 10^{-4}$  to  $2 \times 10^{-4}$  mg/ $\mu$ L) were spread in each experiment. The same precautions as in previous works were taken to allow for the evaporation of the spreading solvent (15 min was allowed to elapse before beginning the isotherm recording) and for the choice of compression rate (0.062 nm<sup>2</sup>·molecule<sup>-1</sup>·min<sup>-1</sup>). Afterward, a surface pressure ( $\pi$ )–area ( $A$ ) isotherm for the monoglyceride was recorded and used as a control. Some experiments were repeated (at least twice). In these cases, the mean deviation was within  $\pm 0.3$  mN/m for the surface pressure and  $\pm 0.05$  m<sup>2</sup>/mg for the area. Then, the monoglyceride monolayer was compressed up to the desired surface pressure (10 mN/m, 20 mN/m, or the collapse point) before experiments for  $\beta$ -lactoglobulin penetration were carried out. For  $\beta$ -lactoglobulin-adsorbed films from water, a protein solution (C $\beta$ -lactoglobulin) at  $1 \times 10^{-4}$  or  $1 \times 10^{-5}$  wt % was left in the trough and time was allowed for protein penetration at the interface. These  $\beta$ -lactoglobulin concentrations were selected from previous data of the adsorption isotherm.<sup>15</sup> At C $\beta$ -lactoglobulin =  $1 \times 10^{-5}$  wt % the surface pressure at equilibrium is zero. In fact, in control experiments, we have observed that for the  $\beta$ -lactoglobulin solution at  $1 \times 10^{-5}$  wt % the surface pressure ( $\pi$ ) at the maximum area of the trough was practically zero after 24 h of adsorption on a clean air–water interface. However, at C $\beta$ -lactoglobulin =  $1 \times 10^{-4}$  wt % the surface pressure at equilibrium is  $\approx 12$  mN/m. For the dynamics of penetration experiments, the  $\beta$ -lactoglobulin solution was added to the aqueous subphase, being injected beyond the barrier, underneath the monolayer. The injection method used for penetration experiments has the disadvantage that the kinetics were limited by the diffusion of the protein in the subphase after injection, and this could result in poor reproducibility or artifacts. To avoid this problem, we built a device that allows fast mixing of the  $\beta$ -lactoglobulin solution in the subphase.<sup>1</sup>

**Surface Film Balance.** Measurements of surface pressure ( $\pi$ )–area ( $A$ ) isotherms of  $\beta$ -lactoglobulin–monoglyceride mixed films at the air–water interface were performed on a fully automated Wilhelmy-type film balance as described previously.<sup>16</sup> These experiments were performed after previous penetration experiments. After the surface pressure had relaxed to a steady-state value the monolayer was expanded up to the maximum area of the trough (at  $\pi = 0$ ), then 60 min was allowed to elapse before beginning the isotherm recording. The  $\pi$ – $A$  isotherm was measured at least three times. The reproduc-

ibility of the results was better than  $\pm 0.5$  mN/m for surface pressure and  $\pm 0.05$  m<sup>2</sup>/mg for area.

**Brewster Angle Microscopy (BAM).** A commercial Brewster angle microscope, BAM2, manufactured by NFT (Göttingen, Germany) was used to study the topography of the monolayer (BAM image and thickness) during dynamic (dynamics of penetration) and static ( $\pi$ – $A$  isotherm recording) measurements. The Brewster angle microscope was positioned over the film balance. Further characteristics of the device and operational conditions have been described elsewhere.<sup>13,14</sup> The surface pressure measurements, area, and gray level as a function of time were carried out simultaneously by means of a device connected between the film balance and the Brewster angle microscope. The imaging conditions were adjusted to optimize both image quality and quantitative measurement of reflectivity. Thus, generally as the surface pressure or the protein content increased the shutter speed was also increased. The reflected beam passes through a focal lens, into an analyzer at a known angle of incident polarization, and finally to a CCD camera. Rotation of the analyzer allows the image contrast to be adjusted by varying the reflected polarization that reaches the camera. If the emulsifier domain does not have a uniform reflectivity this reflectivity changes with the analyzer angle. Thus, the optical anisotropy, which is typical for liquid condensed (LC) structures due to crystalline-like domains being formed at the air–water interface,<sup>13</sup> can be visualized for different positions of the analyzer relative to the plane of incidence. Some images were recorded in absence of the automatic gain control (AGC) in order to distinguish between protein domains (with high reflectivity, which saturate the camera with a completely white image) and monoglyceride domains in a continuous homogeneous phase (with low reflectivity).

**Surface Dilatational Rheology.** To obtain surface rheological parameters, such as surface dilatational modulus, its elastic,  $E_d$ , and viscous,  $E_v$ , components, and the loss angle tangent,  $\tan \theta$ , a modified Wilhelmy-type film balance (KSV 3000) was used as described elsewhere.<sup>16,17</sup> In this method the surface is subjected to small periodic sinusoidal compressions and expansions by means of two oscillating barriers at a given frequency ( $\omega$ ) and amplitude ( $\Delta A/A$ ), and the response of the surface pressure is monitored. Surface pressure was directly measured by means of two roughened platinum plates situated on the surface between the two barriers. The surface dilatational modulus derived from the change in surface pressure resulting from a small change in surface area may be described by the equation:<sup>18</sup>

$$E = - \frac{d\pi}{d \ln A} = E_d + iE_v$$

The dilatational modulus is a complex quantity and is composed of real and imaginary parts. The real part of the dilatational modulus or storage component is the dilatational elasticity,  $E_d = |E| \cos \theta$ . The imaginary part of the dilatational modulus or loss component is the surface dilatational viscous modulus,  $E_v = |E| \sin \theta$ . The loss angle tangent can be defined by  $\tan \theta = E_v/E_d$ . Thus, for a perfectly elastic monolayer  $\tan \theta = 0$ . Measurements were performed at least three times. The reproducibility of these results was better than 5%.

## Results

**Dynamics of the Penetration of  $\beta$ -Lactoglobulin into Spread Monoglyceride Monolayers.** Penetration at a Surface Pressure of 10 mN/m. At initial surface pressures of the monoglyceride spread monolayer ( $\pi_i^{\text{MP}}$  or  $\pi_i^{\text{MO}}$ ) lower than the

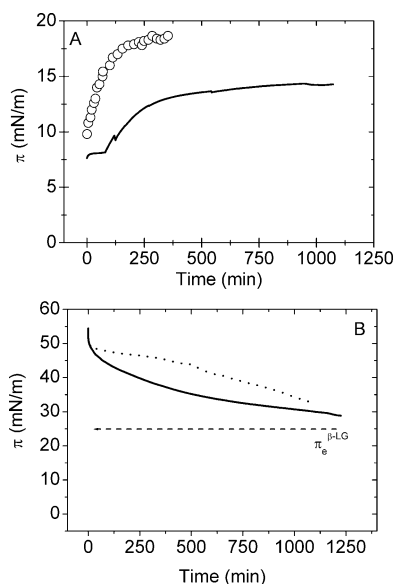


**Figure 1.** Time dependence of surface pressure during the penetration of  $\beta$ -lactoglobulin into a monopalmitin monolayer at an initial surface pressure of (A) 10 mN/m and (B) at the collapse point. Concentration of  $\beta$ -lactoglobulin in the bulk phase (% w/w): (O)  $1 \times 10^{-4}$  and (solid line)  $1 \times 10^{-5}$ . The long-term relaxation of a pure monopalmitin monolayer (dotted line) is included as a reference. The equilibrium spreading pressure of  $\beta$ -lactoglobulin ( $\pi_e^{\beta\text{-LG}}$ ) is indicated by an arrow. Temperature 20 °C.

equilibrium spreading pressure of monopalmitin ( $\pi_e^{\text{MP}} \approx 49.0$  mN/m) or monoolein ( $\pi_e^{\text{MO}} \approx 45.7$  mN/m) and for a concentration of  $\beta$ -lactoglobulin in the bulk phase ( $C_{\beta\text{-lactoglobulin}}$ ) of  $1 \times 10^{-5}$  wt %, the evolution of surface pressure with time after the injection of  $\beta$ -lactoglobulin corresponds to an adsorption mechanism with two kinetic steps (Figures 1A and 2A): (i) initially the surface pressure was constant, and finally, (ii)  $\pi$  increased progressively with the penetration time up to a maximum plateau value. The equilibrium spreading pressure ( $\pi_e$ ) is the maximum surface pressure to which a spread monolayer may be compressed without the possibility of monolayer collapse.

From the results in Figure 1A for monopalmitin it can be seen that for the penetration of  $\beta$ -lactoglobulin into monopalmitin monolayers the initial plateau in the  $\pi$ –time curve at  $\pi_i^{\text{MP}} = 10$  mN/m and at  $C_{\beta\text{-lactoglobulin}} = 1 \times 10^{-5}$  wt % disappears at a higher  $C_{\beta\text{-lactoglobulin}}$  (at  $C_{\beta\text{-lactoglobulin}} = 1 \times 10^{-4}$  wt %), and the maximum surface pressure attained at longer times is higher at the higher  $C_{\beta\text{-lactoglobulin}}$  ( $\approx 18.8$  mN/m) compared to that at lower  $C_{\beta\text{-lactoglobulin}}$  ( $\approx 14.3$  mN/m). For the same amount of  $\beta$ -lactoglobulin injected into the subphase, the surface pressure at equilibrium is 0 and  $\approx 12$  mN/m for  $C_{\beta\text{-lactoglobulin}}$  of  $1 \times 10^{-5}$  and  $1 \times 10^{-4}$  wt %, respectively. Monoolein monolayers penetrated by  $\beta$ -lactoglobulin behave in a similar way (data not shown). Thus, the monoglyceride monolayer (either monopalmitin or monoolein) acts as a promoter of access of  $\beta$ -lactoglobulin at the air–water interface at  $\pi_i^{\text{MONOGLYCERIDE}} < \pi_e^{\text{MONOGLYCERIDE}}$ .

**Penetration at Surface Pressures Higher than the Equilibrium Spreading Pressure of Monoglyceride ( $\pi_e^{\text{MONOGLYCERIDE}}$ ).** At an initial surface pressure higher than the equilibrium spreading pressure of the monoglyceride (at the collapse point of the monoglyceride monolayer),<sup>15</sup> the evolution of surface pressure with time was unexpected, but the same results were observed after repeated experiments with monopalmitin (Figure 1B) or monoolein (Figure 2B). Similar results were also observed for the same monoglycerides with a different protein.<sup>1</sup> It can be

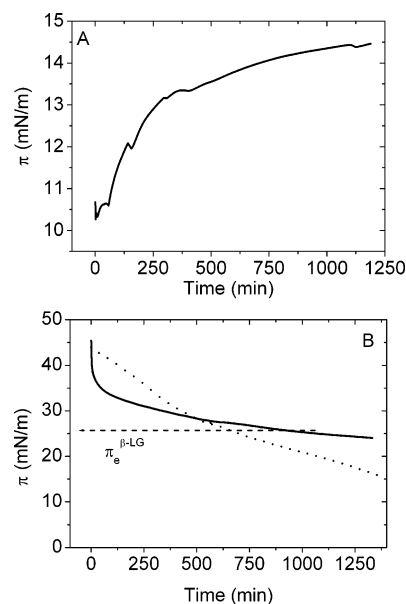


**Figure 2.** Time dependence of surface pressure during the penetration of  $\beta$ -lactoglobulin into a monoolein monolayer at an initial surface pressure of (A) 10 mN/m and (B) at the collapse point. Concentration of  $\beta$ -lactoglobulin in the bulk phase  $1 \times 10^{-5}$  wt %. The long-term relaxation of a pure monoolein monolayer (dotted line) is included as a reference. The equilibrium spreading pressure of  $\beta$ -lactoglobulin ( $\pi_e^{\beta\text{-LG}}$ ) is indicated by an arrow. Temperature 20 °C.

seen that starting the injection of  $\beta$ -lactoglobulin in the aqueous subphase as the monolayer relaxed from the monopalmitin and monoolein collapse (at  $\approx 53$  mN/m and  $\approx 46$  mN/m for monopalmitin and monoolein, respectively), the evolution of surface pressure with time was the opposite of that discussed at  $\pi_i^{\text{MONOGLYCERIDE}} = 10$  mN/m in the preceding section. In fact, it can be seen that as the molecules in monopalmitin or monoolein monolayers are in a state involving the strongest intermolecular interactions, with maximum density packing (with either a solid monopalmitin monolayer or a liquid-expanded monoolein monolayer at the maximum condensation)<sup>13</sup> the surface pressure decreases progressively with the penetration time and tends to a minimum value, which is similar to the  $\pi_e^{\beta\text{-lactoglobulin}}$  value. To gain some insight into these complex dynamic phenomena we have included in Figures 1B and 2B the results of long-term relaxation for pure monopalmitin and monoolein monolayers, respectively, at surface pressures higher than  $\pi_e^{\text{monoglyceride}}$ . It can be seen that after a short relaxation time, at which the relaxation data can be quantified by monolayer collapse, the monolayer molecular loss by desorption controls the monolayer instability at long-term relaxation.<sup>19</sup> Clearly, the collapse and desorption of monoglyceride monolayers explain the penetration of  $\beta$ -lactoglobulin into the spread monoglyceride monolayer at the highest state of condensation, at the collapse point of the spread monolayer.

**Topography of Monoglyceride Monolayers Penetrated by  $\beta$ -Lactoglobulin under Dynamic Conditions.** *Topography of Monoglyceride Monolayers at 10 mN/m.* For a monopalmitin monolayer at  $\pi_i^{\text{MP}} = 10$  mN/m penetrated by  $\beta$ -lactoglobulin the monolayer reflectivity increases with the surface pressure as the penetration process takes place (Figure 3B). The monolayer reflectivity is a maximum at the highest surface pressure at the plateau. The increase in  $I$  with  $\pi$  suggests that an increase in the monolayer thickness from more expanded to more condensed film structure takes place. Interestingly, the reflectivity of some spots of the mixed film is higher than that for pure components, which are included in Figure 3 as a



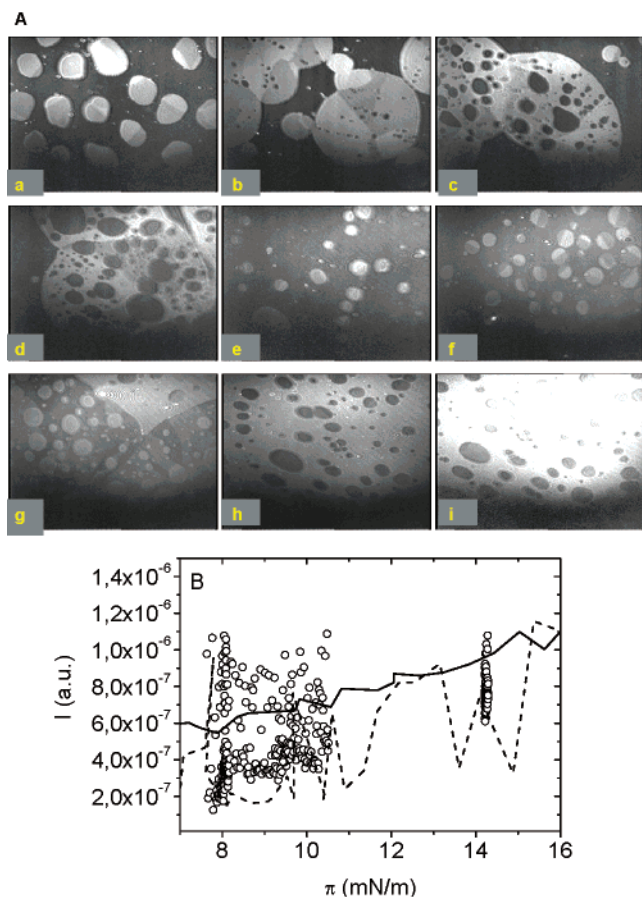


**Figure 3.** (A) Visualization by BAM and (B) reflectivity of monopalmitin monolayers penetrated by  $\beta$ -lactoglobulin as a function of the penetration time and at 20 °C. The initial surface pressure of a spread monopalmitin monolayer is 10 mN/m. The concentration of  $\beta$ -lactoglobulin in the bulk phase is  $1 \times 10^{-5}$  wt %. Key of images in A: (a) time = 0,  $\pi = 12$  mN/m, (b) time = 90 min,  $\pi = 7.7$  mN/m, (c) time = 170 min,  $\pi = 7.5$  mN/m, (d) time = 300 min,  $\pi = 10.5$  mN/m, (e) time = 300 min,  $\pi = 10.5$  mN/m, (f) time = 1200 min,  $\pi = 14.3$  mN/m, (g) time > 1200 min, compression at  $\pi = 24$  mN/m, (h) time > 1200 min, compression at  $\pi = 27$  mN/m, and (i) like image h without AGC. The horizontal direction of the image corresponds to 630  $\mu\text{m}$ , and the vertical direction of the image corresponds to 470  $\mu\text{m}$ . Symbols in B: (solid line)  $\beta$ -lactoglobulin, (dashed line) monopalmitin, and (○) monopalmitin monolayers penetrated by  $\beta$ -lactoglobulin.

reference. These results support the hypothesis that for mixed films of monopalmitin penetrated by  $\beta$ -lactoglobulin some degree of attractive interactions between film forming components does exist at a microscopic level, giving a mixed film with greater thickness as compared with those of pure components. The same phenomenon was observed for  $\beta$ -casein-monopalmitin adsorbed mixed films.<sup>1,7</sup>

At a microscopic level the penetration of  $\beta$ -lactoglobulin into a monopalmitin monolayer gives mixed films with characteristic features (Figure 3A). Briefly, in contrast with the typical circular liquid-condensed (LC) domains of monopalmitin at  $5 < \pi < 30$  mN/m uniformly distributed on the homogeneous liquid-expanded (LE) phase (Figure 3Aa), a mixed film of monopalmitin at  $\pi_i^{\text{MP}} = 10$  mN/m penetrated by  $\beta$ -lactoglobulin may exist with large (Figure 3Ab) and deformed (Figure 3Ac) domains of monopalmitin with a LC structure, and numerous small holes in the interior of the LC monopalmitin domains (Figure 3Ac,d). These holes are probably the nuclei of  $\beta$ -lactoglobulin domains penetrating into large monopalmitin LC domains and may be the cause of the large size of these domains in the mixed film. However, we do not reject the possibility that penetration of

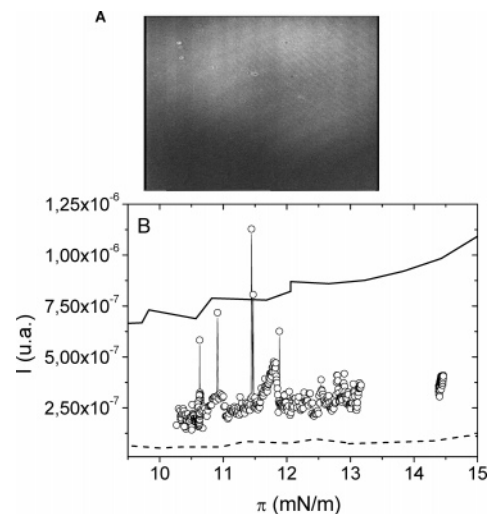


**Figure 4.** (A) Visualization by BAM and (B) reflectivity of monoolein monolayers penetrated by  $\beta$ -lactoglobulin as a function of the penetration time and at 20 °C. The initial surface pressure of a spread monoolein monolayer is 10 mN/m. The concentration of  $\beta$ -lactoglobulin in the bulk phase is  $1 \times 10^{-5}$  wt %. The horizontal direction of the image corresponds to 630  $\mu\text{m}$ , and the vertical direction of the image corresponds to 470  $\mu\text{m}$ . Symbols in B: (solid line)  $\beta$ -lactoglobulin, (dashed line) monoolein, and (○) monoolein monolayers penetrated by  $\beta$ -lactoglobulin.

$\beta$ -lactoglobulin also takes place into the homogeneous region with LE monopalmitin structure. Unfortunately, the homogeneous region of both  $\beta$ -lactoglobulin and LE monopalmitin domains cannot be distinguished by BAM.<sup>17</sup> However, the majority of the interface is covered by small LC domains of monopalmitin distributed uniformly (Figure 3Ae,f), even at the end of the penetration (after 1200 min of  $\beta$ -lactoglobulin penetration). These topographical characteristics prove the existence of few interactions between film-forming components.

The topography of the mixed film of monopalmitin monolayers penetrated by  $\beta$ -lactoglobulin at the end of the penetration (after 1200 min of  $\beta$ -lactoglobulin penetration) and during further compression also demonstrates the presence of large regions of collapsed  $\beta$ -lactoglobulin with LC domains of monopalmitin (Figure 3Ag). After a further compression a continuous phase of collapsed  $\beta$ -lactoglobulin with holes of LC monopalmitin domains was observed (Figure 3Ah). The presence of monopalmitin in the circular holes of Figure 3g,h can be confirmed by changes in the reflectivity with the analyzer angle (data not shown) due to the anisotropy of this phase. On the other hand, the presence of  $\beta$ -lactoglobulin in the continuous phase can also be confirmed by the high brightness as the image is registered in the absence of AGC (Figure 3Ai). In summary, the results reported here suggest that in  $\beta$ -lactoglobulin-monopalmitin mixed films, islands of protein and monoglyceride do exist at the air–water interface. The heterogeneity of the interface is proved by the presence of numerous reflectivity peaks (Figure 3B).

Moreover, the penetration of  $\beta$ -lactoglobulin into a monopalmitin monolayer can be also visualized at a microscopic level by the reduction of mobility of LC monopalmitin domains, which correlates with the higher shear viscosity of  $\beta$ -lactoglobulin and monopalmitin mixed films at the higher surface pressures<sup>20,22</sup> as the penetration process progresses.

The topography of monoolein monolayers at  $\pi_i^{\text{MO}} = 10$  mN/m penetrated by  $\beta$ -lactoglobulin (Figure 4) is essentially different from that of monopalmitin in the mixture (Figure 3). Briefly, (i) the reflectivity of the mixed films is between those

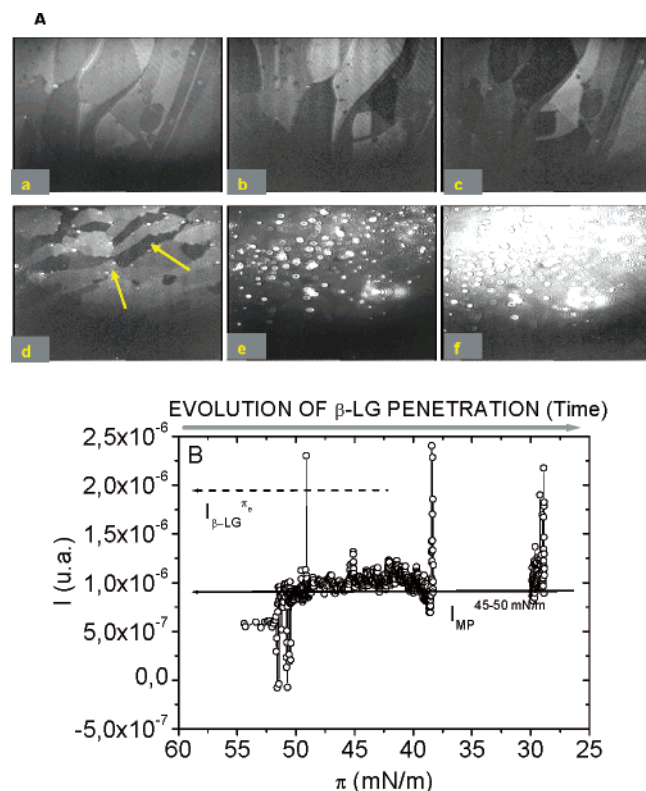


**Figure 5.** (A) Visualization by BAM and (B) reflectivity of monopalmitin monolayers penetrated by  $\beta$ -lactoglobulin as a function of the penetration time and at 20 °C. The initial surface pressure of a spread monopalmitin monolayer coincides with the surface pressure at the collapse point. The reflectivities of monopalmitin and  $\beta$ -lactoglobulin at the respective collapse points are indicated by arrows. The concentration of  $\beta$ -lactoglobulin in the bulk phase is  $1 \times 10^{-5}$  wt %. Key of images in A: (a) time = 240 min,  $\pi = 13.7$  mN/m, and without analyzer, (b) like image a with analyzer at 130°, (c) like image a with analyzer at 60°, (d) time = 1250 min,  $\pi = 28.8$  mN/m (the arrows indicated the nucleus of  $\beta$ -lactoglobulin), (e) time = 1250 min,  $\pi = 28.8$  mN/m, and (f) time = 1250 min,  $\pi = 28.8$  mN/m, in the absence of AGC. Shutter speed 1/250 s. The horizontal direction of the image corresponds to 630  $\mu$ m, and the vertical direction of the image corresponds to 470  $\mu$ m.

of pure components, which are included in Figure 4B as a reference. (ii) The increase in  $I$  with  $\pi$  suggests that an increase in the monolayer thickness from more expanded to more condensed film takes place, but maintaining the same liquid-expanded-like structure of the film forming components. In fact, as expected,<sup>14</sup> the morphology of the interface with pure components and the mixed film is practically identical because in this region both components and the mixed film form an isotropic (homogeneous) monolayer without any difference in the domain topography (Figure 4A). (iii) The reduction of reflectivity peaks (Figure 4B) also proves the existence of a higher degree of homogeneity in the topography of mixed penetrated monolein monolayers compared to mixed penetrated monopalmitin monolayers (Figure 3B).

**Topography of Monoglyceride Monolayers at Surface Pressures Higher than the Equilibrium Spreading Pressure of Monoglyceride ( $\pi_e^{\text{MONOGLYCERIDE}}$ ).** The topography of a monopalmitin monolayer at an initial surface pressure higher than the equilibrium spreading pressure of the monoglyceride (at the collapse point) penetrated by  $\beta$ -lactoglobulin (Figure 5) confirms the conclusions derived from the time evolution of  $\pi$  (Figure 1B). In the same figure the reflectivity of pure components at the respective collapse points are included. It can be seen that starting the injection of  $\beta$ -lactoglobulin in the aqueous subphase,

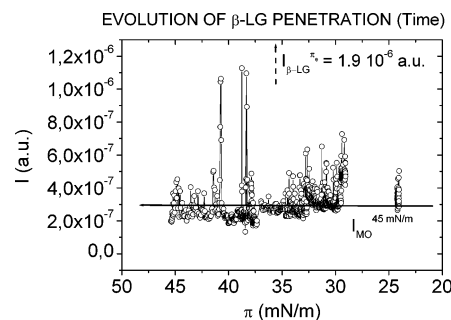


**Figure 6.** Reflectivity of monolein monolayers penetrated by  $\beta$ -lactoglobulin as a function of the penetration time and at 20 °C. The initial surface pressure of a spread monolein monolayer coincides with the surface pressure at the collapse point. The reflectivities of monolein and  $\beta$ -lactoglobulin at the respective collapse points are indicated by arrows. The concentration of  $\beta$ -lactoglobulin in the bulk phase is  $1 \times 10^{-5}$  wt %. Shutter speed 1/50 s. The horizontal direction of the image corresponds to 630  $\mu$ m, and the vertical direction of the image corresponds to 470  $\mu$ m.

at the initial surface pressure of monopalmitin collapse (at  $\pi_i^{\text{MP}} \approx 53$  mN/m), the reflectivity of the interface is lower than that of a pure monopalmitin monolayer but increases as the surface pressure decreases due to the penetration of  $\beta$ -lactoglobulin into the interface. The results shown in Figure 5B also prove that the penetration of  $\beta$ -lactoglobulin into the monopalmitin monolayer does not take place with a collapsed structure because of the reflectivity peaks of the mixed film, which are attributed to  $\beta$ -lactoglobulin domains and are lower than those for a collapsed  $\beta$ -lactoglobulin monolayer (with some exceptions). In fact, it can be seen that as the penetration of  $\beta$ -lactoglobulin into the monopalmitin takes place the reflectivity of the interface is a little higher than that for the pure monopalmitin monolayer but much lower than the reflectivity of a pure  $\beta$ -lactoglobulin collapsed film at  $\pi > \pi_e^{\beta\text{-LG}}$ . Finally, at long-term penetration the reflectivity remains constant. The presence of reflectivity peaks during the penetration proves the heterogeneity of the mixed film and the immiscibility between film forming components with monopalmitin domains (of lower  $I$ ) and  $\beta$ -lactoglobulin-penetrated domains (with higher  $I$ ) distributed at the interface.

The morphology of the interface at the beginning of the penetration process shows the presence of monopalmitin in large regions, as confirmed by the change in the isotropy of the image in the absence of the analyzer (Figure 5Aa) and with the analyzer at angles of 60° (Figure 5Ab) and 130° (Figure 5Ac). However, as the penetration process progresses (at lower surface pressures) small nuclei of  $\beta$ -lactoglobulin (Figure 5Ad) and regions with small domains of monopalmitin (Figure 5Ae) over a thick sublayer of  $\beta$ -lactoglobulin with high reflectivity in the absence of AGC (Figure 5Af) can be clearly distinguished throughout the interface. The penetration of  $\beta$ -lactoglobulin into a monopalmitin monolayer can be also visualized at a microscopic level by the reduction of mobility in LC monopalmitin domains as the penetration process progresses, which correlates with the higher shear viscosity of  $\beta$ -lactoglobulin compared to monopalmitin monolayers.<sup>21</sup>

Similar results are observed for the evolution of the reflectivity of a monolein monolayer penetrated by  $\beta$ -lactoglobulin (Figure 6). However, the morphology of the mixed films is similar to that of pure components because in this region both components and the mixed film form a monolayer with a liquid-expanded-like structure (see Figure 4A). The presence of reflectivity peaks (Figure 6) also proves the heterogeneous topography of mixed penetrated films due to the presence of

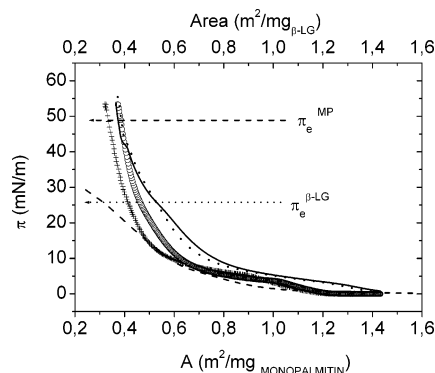


**Figure 7.** Surface pressure isotherms (compression curve) for mixed monolayers of monopalmitin penetrated by  $\beta$ -lactoglobulin at  $1 \times 10^{-5}$  % w/w in buffered water at pH 7 and at 20 °C. Initial surface pressure of a monopalmitin monolayer before the injection of  $\beta$ -lactoglobulin into the aqueous phase: (solid line) 10 mN/m, (dotted line) 20 mN/m, and (+) at the collapse point. The  $\pi$ - $A$  isotherms for pure (dashed line)  $\beta$ -lactoglobulin and (O) monopalmitin monolayers are included as reference. The  $\pi_e$  of  $\beta$ -lactoglobulin is indicated by means of an arrow.

domains of  $\beta$ -lactoglobulin (with high  $I$ ) and LE domains of monoolein (with low  $I$ ).

**Structural Characteristics of Monoglyceride Monolayers Penetrated by  $\beta$ -Lactoglobulin.** *Structural Characteristics of Monopalmitin Monolayers Penetrated by  $\beta$ -Lactoglobulin.* The  $\pi$ - $A$  isotherms for monopalmitin monolayers penetrated by  $\beta$ -lactoglobulin on the basis that only monopalmitin was present at the interface ( $A$ ,  $\text{m}^2/\text{mg}_{\text{MP}}$ ) at different  $\pi_i^{\text{MP}}$  and at 20 °C, are shown in Figure 7. In the same figure we have included the  $\pi$ - $A$  isotherms for a spread monopalmitin monolayer registered at the beginning of each experiment and for an adsorbed  $\beta$ -lactoglobulin monolayer, which can be used as a control and for comparison, respectively. The  $\pi$ - $A$  isotherms for pure spread monopalmitin<sup>13</sup> and adsorbed  $\beta$ -lactoglobulin<sup>21</sup> monolayers are in good agreement with data in the literature.

The results of the  $\pi$ - $A$  isotherms (Figure 7) with the help of the compressional coefficient (data not shown) deduced from the slope of the  $\pi$ - $A$  isotherm ( $\kappa = -d\pi/dA$ ) indicate that adsorbed  $\beta$ -lactoglobulin monolayers at the air-water interface adopt a liquid expanded-like structure and the collapse phase. However, according to Graham and Phillips,<sup>23</sup>  $\beta$ -lactoglobulin retains elements of the native structure, not fully unfolded at the interface. Thus, most amino acid residues in  $\beta$ -lactoglobulin adopt loop conformation at the air-water interface. But the loop conformation is more condensed at higher surface pressures and is displaced toward the bulk phase at the collapse point. The monolayer collapses at a surface pressure of  $\approx 30$  mN/m (Figure 7), a value close to  $\pi_e^{\beta\text{-LG}}$ , which is indicated in Figure 7 by an arrow.

Monopalmitin spread monolayers show a rich structural polymorphism as a function of surface pressure (Figure 7). The liquid-expanded (LE) phase (at  $\pi < 5$  mN/m), an intermediate region at the broad plateau due to a degenerated first-order phase transition between liquid-condensed (LC) and liquid-expanded structures (at  $5 < \pi < 30$  mN/m), the liquid-condensed structure (at  $\pi > 30$  mN/m), and finally, the solid (S) structure near to the monolayer collapse at a surface pressure of about 53.1 mN/m were observed. That is, monopalmitin monolayers are in a metastable state at  $\pi > \pi_e^{\text{MP}} \approx 49$  mN/m.

For monopalmitin spread monolayers penetrated by  $\beta$ -lactoglobulin at different  $\pi_i^{\text{MP}}$  it can be seen (Figure 7) that, on the basis that only monopalmitin was present at the interface, the  $\pi$ - $A$  isotherms for monopalmitin and for  $\beta$ -lactoglobulin-

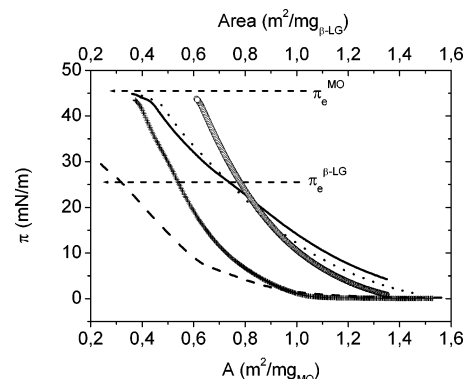


**Figure 8.** Surface pressure isotherms (compression curve) for mixed monolayers of monoolein penetrated by  $\beta$ -lactoglobulin at  $1 \times 10^{-5}$  % (w/w) in buffered water at pH 7 and at 20 °C. Initial surface pressure of a monoolein monolayer before the injection of  $\beta$ -lactoglobulin into the aqueous phase: (solid line) 10 mN/m, (dotted line) 20 mN/m, and (+) at the collapse point. The  $\pi$ - $A$  isotherms for pure (dashed line)  $\beta$ -lactoglobulin and (O) monoolein monolayers are included as reference. The  $\pi_e$  of  $\beta$ -lactoglobulin is indicated by means of an arrow.

monopalmitin mixed monolayers at  $\pi_i^{\text{MP}} < \pi_e^{\text{MP}}$  are practically coincident. That is, the structures of the mixed monolayers are practically dominated by the presence of monopalmitin. In fact, the first-order transition between LC and LE structures (at  $\pi \approx 5$  mN/m) can be distinguished, which is typical of a pure monopalmitin monolayer. In addition, the mixed film collapsed at the collapse pressure of a pure monopalmitin monolayer. However, in the range of existence of an adsorbed  $\beta$ -lactoglobulin monolayer (at  $\pi < \pi_e^{\beta\text{-LG}}$ ) the  $\pi$ - $A$  isotherms for  $\beta$ -lactoglobulin and for  $\beta$ -lactoglobulin-monopalmitin mixed monolayers are different. These results suggest that at  $\pi > \pi_e^{\beta\text{-LG}}$  protein displacement by the monoglyceride from the air-water interface takes place. At  $\pi < \pi_e^{\beta\text{-LG}}$  both  $\beta$ -lactoglobulin and monopalmitin may coexist at the interface, but the structural characteristics of the mixed monolayers are dominated by the presence of monopalmitin. The only minor difference between monopalmitin and  $\beta$ -lactoglobulin-monopalmitin mixed monolayers is that in the latter the structure is more expanded, because the  $\pi$ - $A$  isotherms are displaced toward higher areas (Figure 7). However, at  $\pi_i^{\text{MP}} = \pi_e^{\text{MP}}$ , although the structures of the mixed monolayers are practically dominated by the presence of monopalmitin, the  $\pi$ - $A$  isotherms are parallel to that of a pure monopalmitin monolayer but displaced toward lower mass areas, which denotes a previous irreversible monopalmitin molecular loss. BAM images and the evolution of the reflectivity of the interface with the surface pressure (data not shown) corroborate at a microscopic level these conclusions.

*Structural Characteristics of Monoolein Monolayers Penetrated by  $\beta$ -Lactoglobulin.* The  $\pi$ - $A$  isotherms for monoolein monolayers penetrated by  $\beta$ -lactoglobulin on the basis that only monoolein was present at the interface ( $A$ ,  $\text{m}^2/\text{mg}_{\text{MO}}$ ) at different  $\pi_i^{\text{MO}}$  and at 20 °C are shown in Figure 8. In the same figure we have included the  $\pi$ - $A$  isotherms for a spread monoolein monolayer registered at the beginning of each experiment and for an adsorbed  $\beta$ -lactoglobulin monolayer. The  $\pi$ - $A$  isotherm for pure spread monoolein monolayer is in good agreement with data in the literature.<sup>13</sup> In contrast to monopalmitin, the monoolein monolayer presents only the LE structure and collapses at the equilibrium spreading pressure ( $\pi_e^{\text{MO}} \approx 45.7$  mN/m).

For monoolein spread monolayers penetrated by  $\beta$ -lactoglobulin at different  $\pi_i^{\text{MO}}$  (Figure 8) it can be seen that, on the basis that only monoolein was present at the interface, the  $\pi$ - $A$



isotherms for pure monoolein and  $\beta$ -lactoglobulin monolayers are different from those for  $\beta$ -lactoglobulin–monoolein mixed monolayers. That is, although pure and mixed monolayers present the same liquid-expanded-like structure, the  $\pi$ – $A$  isotherms for  $\beta$ -lactoglobulin–monoolein mixed monolayers are displaced in relation to pure monolayer components. Interestingly, in the more expanded structure (at  $\pi < \pi_e^{\beta\text{-LG}}$ ) the  $\pi$ – $A$  isotherms for  $\beta$ -lactoglobulin–monoolein mixed monolayers are coincident with those for a pure monoolein monolayer for  $\pi_i^{\text{MO}} < \pi_e^{\text{MO}}$ , but the  $\pi$ – $A$  isotherm of the mixed film coincides with that for a pure  $\beta$ -lactoglobulin monolayer for  $\pi_i^{\text{MO}} = \pi_e^{\text{MO}}$ . At  $\pi_i^{\text{MO}} = \pi_e^{\text{MO}}$  the  $\pi$ – $A$  isotherms for  $\beta$ -lactoglobulin–monoolein mixed monolayers are displaced toward lower monolayer mass areas, as compared with a pure monoolein monolayer. These results suggest that the monoolein monolayer molecular loss due to collapse and/or desorption that takes place during the preceding penetration experiments is irreversible. In fact, the displacement of  $\pi$ – $A$  isotherms for  $\beta$ -lactoglobulin–monoolein mixed monolayers toward lower monolayer mass areas is more intense as  $\pi_i^{\text{MO}}$  increases, especially at the collapse point, in agreement with long-term relaxation data for a pure monoolein monolayer.<sup>19</sup>

**Surface Dilatational Characteristics of Monoglyceride Monolayers Penetrated by  $\beta$ -Lactoglobulin.** Changes in surface dilatational modulus ( $E$ ) and loss angle tangent ( $\tan \theta$ ) for monopalmitin and monoolein spread monolayers penetrated by  $\beta$ -lactoglobulin at different monoglyceride initial surface pressures (at  $\pi_i^{\text{MP}}$  and  $\pi_i^{\text{MO}}$ ), at an amplitude of deformation of 5% and at 20 °C, are shown in Figures 9 and 10, respectively. The percentage area change was determined in preliminary experiments to be in the linear region. In the same figures we have included the evolution of  $E$  with surface pressure for pure monopalmitin and monoolein monolayers at the same amplitude and at a frequency of 50 mHz.<sup>27</sup>

It can be seen that  $E$  and  $\tan \theta$  increase with frequency and tend to a plateau at the higher frequencies (Figures 9 and 10). This behavior corroborates the conclusion that the surface dilatational characteristics of mixed monolayers of monoglyceride penetrated by  $\beta$ -lactoglobulin are practically viscoelastic.

Surprisingly, although the surface pressures at the end of the penetration process, which coincides with the beginning of the surface dilatational experiments, are a little lower for monopalmitin than for monoolein monolayers penetrated by  $\beta$ -lactoglobulin (Figures 1 and 2), the values of  $E$  are higher for monopalmitin (Figure 9A) than for monoolein (Figure 10A). In addition, the values of  $E$  also increase with  $\pi_i^{\text{MP}}$  and  $\pi_i^{\text{MO}}$ , for monopalmitin and for monoolein monolayers penetrated by  $\beta$ -lactoglobulin. However, the concentration of  $\beta$ -lactoglobulin injected into the subphase, which has a significant effect on the dynamics of penetration (Figure 1A), does not affect the surface dilatational characteristics of the mixed film (Figure 9).

At the same frequency (at 50 mHz) for mixed monolayers of monopalmitin penetrated by  $\beta$ -lactoglobulin (Figure 9A), (i) the values of  $E$  at  $\pi_i^{\text{MP}} = 10$  mN/m are the same as those for  $\beta$ -lactoglobulin but higher than those for monopalmitin, (ii) at  $\pi_i^{\text{MP}} = 20$  mN/m the values of  $E$  are the same as those for monopalmitin, but higher than those for  $\beta$ -lactoglobulin, and (iii) at  $\pi_i^{\text{MP}} = \pi_e^{\text{MP}}$  the values of  $E$  are lower than those for monopalmitin, but higher than those for  $\beta$ -lactoglobulin. However, for monoolein monolayers penetrated by  $\beta$ -lactoglobulin (Figure 10A) the values of  $E$  are lower than those for pure monolayer components. A monoolein monolayer penetrated by  $\beta$ -lactoglobulin at  $\pi_i^{\text{MO}} = 10$  mN/m is an exception because

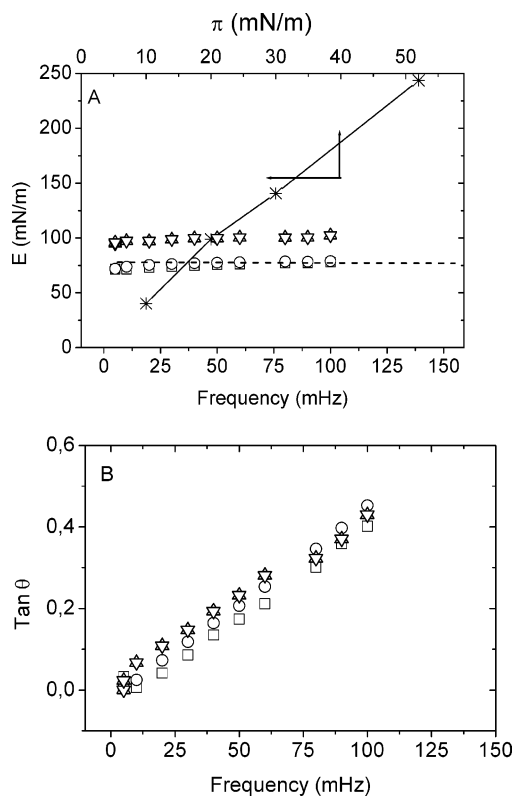


**Figure 9.** Frequency dependence of (A) surface dilatational modulus and (B) loss angle tangent for mixed monolayers of monopalmitin penetrated by  $\beta$ -lactoglobulin at pH 7 and at 20 °C. Initial surface pressure of a monopalmitin monolayer before the injection of  $\beta$ -lactoglobulin into the aqueous phase: ( $\square$ ) 10 mN/m and  $\beta$ -lactoglobulin at  $1 \times 10^{-4}$  % (w/w) into the aqueous phase, ( $\circ$ ) 10 mN/m and  $\beta$ -lactoglobulin at  $1 \times 10^{-5}$  % (w/w) into the aqueous phase, ( $\triangle$ ) 20 mN/m and  $\beta$ -lactoglobulin at  $1 \times 10^{-5}$  % (w/w) into the aqueous phase, and ( $\nabla$ ) at the collapse point and  $\beta$ -lactoglobulin at  $1 \times 10^{-5}$  % (w/w) into the aqueous phase. The surface pressure dependence of surface dilatational modulus for pure (\*) monopalmitin and (dashed line)  $\beta$ -lactoglobulin monolayers at a frequency of 50 mHz are included as a reference.

$E$  values for the mixed film and for a pure monoolein monolayer are the same (Figure 10A).

## Discussion

In this work we have used complementary interfacial techniques (dynamic tensiometry, surface film balance, BAM, and surface dilatational rheology) to analyze the penetration of  $\beta$ -lactoglobulin into a monoglyceride monolayer (monopalmitin or monoolein) spread at the air–water interface under dynamic (dynamics of penetration) and static (structural, topographical, and dilatational characteristics) conditions.

The dynamics of penetration of  $\beta$ -lactoglobulin into a monoglyceride monolayer was followed by measurements of the time evolution of surface pressure at a constant surface area.  $\beta$ -Lactoglobulin was injected into the aqueous bulk phase, underneath the monopalmitin (Figure 1) or monoolein (Figure 2) monolayer, at different initial surface pressures (at  $\pi_i^{\text{MP}}$  or  $\pi_i^{\text{MO}}$ , respectively). It was observed that the dynamics of surface pressure evolution after the injection of  $\beta$ -lactoglobulin into the aqueous bulk phase, underneath the monoglyceride monolayer, depend on the level of initial surface pressure of the spread monoglyceride monolayer ( $\pi_i^{\text{MONOGLYCERIDE}}$ ). The differences observed in the  $\pi$ –time plot as a function of the monoglyceride and  $\pi_i^{\text{MONOGLYCERIDE}}$  suggest that the penetration of  $\beta$ -lactoglobulin is sensitive to the state of condensation of the

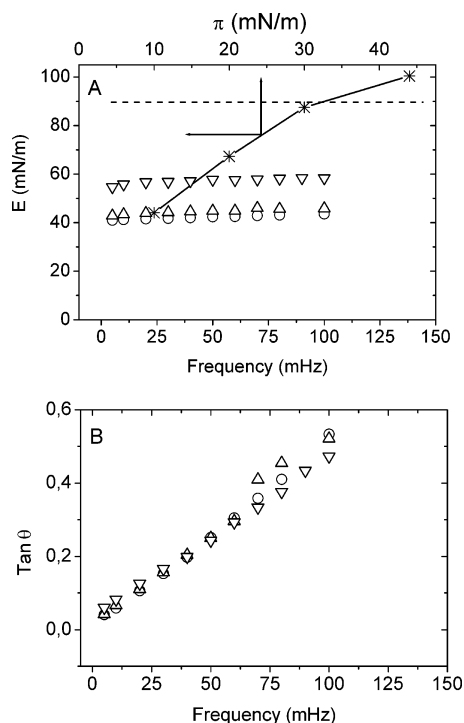


**Figure 10.** Frequency dependence of (A) surface dilatational modulus and (B) loss angle tangent for mixed monolayers of monoolein penetrated by  $\beta$ -lactoglobulin at  $1 \times 10^{-5}$  % (w/w) into the aqueous phase, at pH 7 and at 20 °C. Initial surface pressure of a monopalmitin monolayer before the injection of  $\beta$ -lactoglobulin into the aqueous phase: (○) 10 mN/m, (△) 20 mN/m, and (▽) at the collapse point. The surface pressure dependence of surface dilatational modulus for pure (\*) monoolein and (dashed line)  $\beta$ -lactoglobulin monolayers at a frequency of 50 mHz are included as a reference.

monoglyceride monolayer and, to a lesser degree, depends on the particular monoglyceride. Significant differences can be observed if  $\pi_i^{\text{MONOGLYCERIDE}}$  is lower or higher than the equilibrium spreading pressure of the monoglyceride ( $\pi_e^{\text{MONOGLYCERIDE}}$ ). As stated previously, the equilibrium spreading pressure ( $\pi_e$ ) is the maximum surface pressure to which a spread monolayer may be compressed without the possibility of monolayer collapse.  $\beta$ -Lactoglobulin ( $\pi_e^{\beta\text{-LG}} \approx 25.9$  mN/m) and monoolein ( $\pi_e^{\text{MO}} \approx 45.7$  mN/m) collapse at  $\pi_e$ , while monopalmitin ( $\pi_e^{\text{MP}} \approx 49.0$  mN/m) collapses at  $\pi_e > \pi_e$  (Figures 7 and 8).

At  $\pi_i^{\text{MONOGLYCERIDE}} < \pi_e^{\text{MONOGLYCERIDE}}$  and at the beginning of the penetration, a initial plateau in the  $\pi$ -time plots was observed (Figure 2A), which may be associated with the penetration of  $\beta$ -lactoglobulin from underneath the monoglyceride monolayer, which produces an accumulation of the protein. This finally destabilizes the monoglyceride monolayer and promotes a progressive penetration of  $\beta$ -lactoglobulin into the monoglyceride monolayer at long-term penetration. As a consequence of the  $\beta$ -lactoglobulin penetration into the monoglyceride monolayer the surface pressure increases up to the final maximum plateau value of  $\approx 14.3$  and 14.5 mN/m for monopalmitin and monoolein, respectively. Thus, although the equilibrium surface pressure for the adsorption of  $\beta$ -lactoglobulin at  $C_{\beta\text{-lactoglobulin}} = 1 \times 10^{-5}$  wt % is zero, the protein has the capacity to penetrate into a monoglyceride monolayer at  $\pi_i^{\text{MP}} = \pi_i^{\text{MO}} = 10$  mN/m (similar results have been observed for  $\pi_i^{\text{MP}} = \pi_i^{\text{MO}} = 20$  mN/m). The penetration of  $\beta$ -lactoglobulin is facilitated at higher concentrations in the bulk phase (at  $C_{\beta\text{-lactoglobulin}} = 1 \times 10^{-4}$  wt %) because the initial plateau in the  $\pi$ -time disappears (Figure 1A). From these experiments we

must reject the possibility that a change in the monoglyceride monolayer structure may be produced as a consequence of the penetration of  $\beta$ -lactoglobulin at the interface, as observed for phospholipids at low surface pressures,<sup>24–26</sup> because in the range of surface pressures attained (Figures 1A and 2A) the monopalmitin monolayer is in the region of liquid condensed-liquid expanded transition and monoolein adopts a liquid expanded structure.<sup>13</sup> However, we must not reject the possibility that a change in the monoglyceride monolayer condensation may be produced, maintaining the monolayer structure constant, as a consequence of the penetration of  $\beta$ -lactoglobulin at the interface.

At  $\pi_i^{\text{MONOGLYCERIDE}} > \pi_e^{\text{MONOGLYCERIDE}}$ , the results shown in Figures 1B and 2B for monopalmitin and monoolein, respectively, may be explained by the concurrence of a complex competition between the instability of the monoglyceride monolayer, which causes monolayer molecular loss by collapse and/or desorption,<sup>19</sup> and the penetration of the protein into the interface.<sup>1</sup> In fact, it was observed that at surface pressures higher than  $\pi_e^{\text{MONOGLYCERIDE}}$ , the relaxation phenomena are different for monopalmitin than for monoolein monolayers. For monopalmitin monolayers the relaxation phenomena may be due to monolayer collapse by nucleation and growth of critical nuclei until the  $\pi_e$  value of monopalmitin is attained, followed by a monolayer molecular loss by desorption at long-term relaxation time. For monoolein monolayers and after a short relaxation time, at which the relaxation data can be quantified by monolayer collapse, the monolayer molecular loss by desorption controls the monolayer instability.<sup>19</sup> Clearly, the collapse and desorption of monopalmitin and monoolein monolayers explain the penetration of  $\beta$ -lactoglobulin into the spread monoglyceride monolayer at the highest state of condensation, at the collapse point of the spread monolayer. That is, monoglyceride molecules that desorb from the interface increase the available area so that the  $\beta$ -lactoglobulin molecules will have greater access to penetrate at the interface. A prerequisite for this penetration competition for the interface is the absence of interactions between monoglyceride and  $\beta$ -lactoglobulin molecules, as was confirmed for spread<sup>13,14</sup> and adsorbed<sup>21</sup>  $\beta$ -lactoglobulin–monoglyceride mixed films.

BAM images and the evolution of reflectivity ( $I$ ) during the penetration of  $\beta$ -lactoglobulin into a monoglyceride monolayer as a function of the initial surface pressure of the monoglyceride (Figures 3–6) give support to the conclusions derived from the dynamics of surface pressure evolution with time (Figures 1 and 2). The increase of  $\pi$  with the penetration time is followed by an increase in  $I$  with  $\pi$ , which suggests that an increase in the monolayer thickness from more expanded to more condensed film structure takes place. Although the morphology and reflectivity support evidence that film forming components are present at the interface in isolated domains of monoglyceride (with low  $I$ ) and  $\beta$ -lactoglobulin with (high  $I$ ) with few interactions between them, some degree of attractive interactions is also observed because the reflectivity of some spots of the mixed film is higher than that for pure components. However, the presence of reflectivity peaks proves the heterogeneous topography of mixed penetrated films no matter what the monoglyceride or its initial surface pressure.

The  $\beta$ -lactoglobulin penetration into a monoglyceride monolayer at  $\pi_i^{\text{MONOGLYCERIDE}} < \pi_e^{\text{MONOGLYCERIDE}}$  or the combination of  $\beta$ -lactoglobulin penetration and monoglyceride monolayer molecular loss at  $\pi_i^{\text{MONOGLYCERIDE}} > \pi_e^{\text{MONOGLYCERIDE}}$  has an effect on the structural and rheological characteristics of the mixed films of monoglyceride penetrated by  $\beta$ -lactoglobulin.



The  $\pi$ -A isotherms of monoglyceride monolayers penetrated by  $\beta$ -lactoglobulin were registered after the penetration experiments. At the end of each penetration experiment the monolayer was expanded at the maximum area (at  $\pi \approx 0$  mN/m) and a waiting time of 60 min was allowed before the monolayer compression. From the  $\pi$ -A isotherms for monopalmitin and monoolein mixed monolayers penetrated by  $\beta$ -lactoglobulin (Figures 7 and 8) significant differences between structural characteristics of mixed films depending on the monoglyceride (either monopalmitin or monoolein)  $\pi_i^{\text{MONOGLYCERIDE}}$  can be observed.


Although  $\beta$ -lactoglobulin molecules have the capacity to penetrate a spread monoglyceride monolayer, monoglyceride molecules have the capacity to reenter the monolayer after the expansion and recompression of the mixed monolayer. As monoglyceride reenters the air-water interface the structure of  $\beta$ -lactoglobulin-monoglyceride mixed monolayers is practically dominated by the presence of monoglyceride. These results also suggest that the monoglyceride molecular loss by collapse and/or desorption (deduced in the previous section from dynamic surface pressure measurements) is reversible for monopalmitin at  $\pi_i^{\text{MP}} < \pi_e^{\text{MP}}$  but irreversible at  $\pi_i^{\text{MP}} \geq \pi_e^{\text{MP}}$ . However, for monoolein the molecular loss by collapse and/or desorption at every  $\pi_i^{\text{MO}}$  is irreversible.

For a monoglyceride monolayer penetrated by  $\beta$ -lactoglobulin at a fixed initial surface pressure (at  $\pi_i^{\text{MP}}$  or  $\pi_i^{\text{MO}}$ ) and at  $\pi > \pi_e^{\beta\text{-LG}}$  we deduced from the  $\pi$ -A isotherm that protein displacement by monoglyceride from the air-water interface takes place. However, at  $\pi < \pi_e^{\beta\text{-LG}}$  both  $\beta$ -lactoglobulin and monoglyceride may coexist at the interface. The evolution of the reflectivity of the interface with the surface pressure (data not shown) corroborates at a microscopic level these conclusions.

The frequency dependence of the surface dilatational properties (Figures 9 and 10) may be associated with the effect of the rate of deformation on the structure and relaxation phenomena in the mixed monolayers. The viscoelastic behavior observed for mixed monolayers in the range of frequencies studied may be associated with the organization/reorganization of monolayer structure and with the formation/destruction of protein multilayers and/or monoglyceride collapse, especially at high  $\pi_i^{\text{MP}}$  and  $\pi_i^{\text{MO}}$ . The reason for this behavior must be associated with the immiscibility between monolayer components at the air-water interface, as was observed for  $\beta$ -lactoglobulin-monoglyceride spread mixed monolayers.<sup>28</sup>

From the surface dilatational characteristics of the mixed films it can be concluded that (i) although the monoglyceride monolayer is penetrated by  $\beta$ -lactoglobulin the presence of the monoglyceride (monopalmitin or monoolein) has an effect on the value of  $E$  of the mixed film. These results support the hypothesis that the monoglyceride molecules that are displaced during the preceding penetration experiments may be located near the interface, in agreement with the conclusions derived from the structural characteristics of the mixed films in the preceding section. (ii) The lower values of  $E$  for the mixed films compared to those for a pure monopalmitin monolayer at the collapse point or monoolein monolayers at every  $\pi_i^{\text{MO}}$  are due to monolayer molecular loss, as deduced from experiments on the dynamics of penetration (dynamic surface pressure) and BAM (dynamic topographical characteristics) in preceding sections. (iii) The fact that the  $E$  values are higher for monopalmitin than for monoolein monolayers penetrated by  $\beta$ -lactoglobulin also confirms both that the dilatational characteristics of the mixed monolayers depend on the monoglyceride

**TABLE 1: Penetration of Monoglycerides (monopalmitin and monoolein) by Proteins ( $\beta$ -Lactoglobulin and  $\beta$ -Casein)**

	$\beta$ -Casein-monoglyceride	$\beta$ -Lactoglobulin-monoglyceride
<b>DYNAMIC OF PENETRATION</b>  $\pi_i < \pi_e$ MONOGLYCERIDE	$\pi^{\text{long-term penetration}} \cong \pi_e^{\beta\text{-C}}$ $\downarrow$ $\beta$ -Casein saturate the interface. Molecular loss is reversible for monopalmitin, but irreversible for monoolein	$\pi^{\text{long-term penetration}} < \pi_e^{\beta\text{-LG}}$  $\downarrow$ Penetration requires a previous desorption of the monoglyceride.
$\pi_i > \pi_e$ MONOGLYCERIDE	$\pi^{\text{long-term penetration}} \cong \pi_e^{\beta\text{-C}}$ $\downarrow$ $\beta$ -Casein saturate the interface. Molecular loss is irreversible for monopalmitin and monoolein	$\pi^{\text{long-term penetration}} < \pi_e^{\beta\text{-LG}}$ $\downarrow$ Penetration requires a previous desorption of the monoglyceride.
<b>TOPOGRAPHY</b>	Monoglyceride penetration is easier for $\beta$ -casein than for $\beta$ -lactoglobulin.	
<b>Reflectivity</b>	Monoglyceride and $\beta$ -casein domains are more segregated	
<b>Morphology</b>	Monoglyceride and $\beta$ -lactoglobulin domains are more uniform	
<b>PROTEIN-MONOGLYCERIDE MIXED MONOLAYERS</b>		
<b>STRUCTURE</b>		
$\pi < \pi_e^{\text{PROTEIN}}$	Protein and monoglyceride may coexist at the interface	
$\pi > \pi_e^{\text{PROTEIN}}$	Protein can be squeezed out by the monoglyceride Mixed films are essentially dominated by the monoglyceride	
<b>DILATATIONAL PROPERTIES</b>	At every surface pressures $E$ is higher for $\beta$ -casein- than for $\beta$ -lactoglobulin-monoglyceride mixed films.	
		
$\rightarrow$ Penetration of monoglyceride (monopalmitin or monoolein) is easier for $\beta$ -casein than for $\beta$ -lactoglobulin.		
$\rightarrow$ The more expanded monoolein monolayer and monolayer molecular loss facilitate the penetration of proteins compared to monopalmitin.		

and, furthermore, the immiscibility between monolayer forming components, because the same behavior was observed for pure monoglyceride<sup>27</sup> and for spread mixed<sup>28</sup> monolayers at the air-water interface. (iv) Finally, the viscoelasticity does not depend on the composition of the mixed film nor on the initial surface pressure of the monoglyceride monolayer because the same frequency dependence of  $\tan \theta$  is observed for monopalmitin and monoolein monolayers penetrated by  $\beta$ -lactoglobulin (Figures 9B and 10B, respectively).

In a preceding paper we have analyzed the penetration of  $\beta$ -casein into a monoglyceride monolayer (monopalmitin or monoolein) spread at the air-water interface and its effects on the structural, dilatational, and topographical characteristics of mixed films.<sup>1</sup> From the comparison of the results we can confirm<sup>12</sup> that globular (this work) and disordered<sup>1</sup> proteins can penetrate into monoglyceride<sup>1</sup> and phospholipid<sup>11,12,29</sup> monolayers. However, the effects of the penetration on the structural, dilatational, and topographical characteristics of mixed films depend on the particular protein-lipid (phospholipid) system (Table 1, Figure 11). At every state of the monoglyceride monolayer the penetration is facilitated for  $\beta$ -casein compared to  $\beta$ -lactoglobulin.

(i) In fact, at  $\pi_i^{\text{MONOGLYCERIDE}} < \pi_e^{\text{MONOGLYCERIDE}}$  the penetration of  $\beta$ -casein saturates the interface because at long penetration time the surface pressure tends to a maximum plateau value that coincides with the equilibrium surface pressure for  $\beta$ -casein.<sup>1</sup> However, during the penetration of  $\beta$ -lactoglobulin the surface pressure at the maximum plateau value is lower than  $\pi_e^{\beta\text{-LG}}$  (Figures 1A and 2A).

(ii) At  $\pi_i^{\text{MONOGLYCERIDE}} > \pi_e^{\text{MONOGLYCERIDE}}$  the surface pressure tends to a maximum plateau value during the penetra-

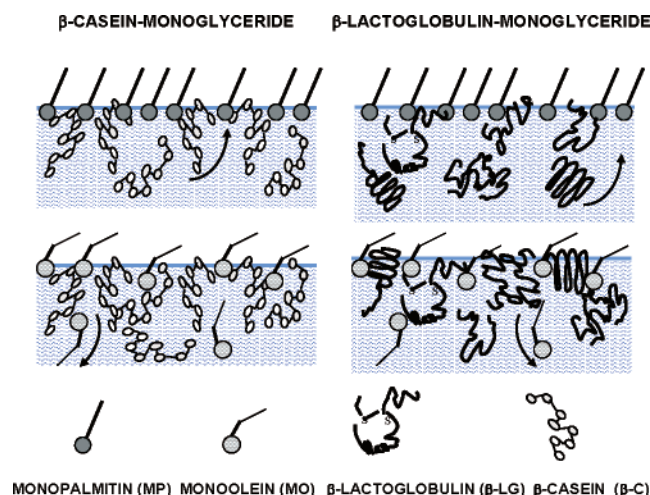


**Figure 11.** Schematic illustration of the differences in the penetration of  $\beta$ -lactoglobulin ( $\beta$ -LG) or  $\beta$ -casein ( $\beta$ -C) into monopalmitin (MP) or monoolein (MO) spread monolayers. The arrows indicated the penetration of the protein or the desorption of the monoglyceride.

tion of  $\beta$ -casein after the monoglyceride molecular loss by collapse—desorption, and finally,  $\beta$ -casein saturates the interface because at long penetration time the surface pressure coincides with the equilibrium spreading pressure for  $\beta$ -casein.<sup>1</sup> However, during the penetration of  $\beta$ -lactoglobulin the surface pressure at the maximum plateau value is lower than  $\pi_e^{\beta$ -LG and requires a previous relaxation of the monoglyceride to low surface pressures before the penetration of  $\beta$ -lactoglobulin takes place (Figures 1B and 2B).

(iii) The surface pressure evolution of the reflectivity also corroborates that the penetration is easier for  $\beta$ -casein<sup>1</sup> than for  $\beta$ -lactoglobulin (Figures 3–6). However, minor differences were observed in the morphology of mixed films penetrated by  $\beta$ -casein<sup>1</sup> and  $\beta$ -lactoglobulin (Figures 3–5).

(iv) Although protein molecules ( $\beta$ -casein and  $\beta$ -lactoglobulin) have the capacity to penetrate into a spread monoglyceride monolayer (monopalmitin or monoolein), monoglyceride molecules have also the capacity to reenter the monolayer after the expansion and recompression of the mixed monolayer, as confirmed by the structural and dilatational characteristics of mixed protein—monoglyceride monolayers. For these systems one may conclude that at surface pressures lower than the equilibrium spreading pressure of the protein ( $\pi_e^{\beta$ -CS or  $\pi_e^{\beta$ -LG) both protein and monoglyceride may coexist at the interface. At higher surface pressures, protein can be squeezed out and the interfacial characteristics of the mixed film are essentially dominated by the presence of monoglyceride (either monopalmitin or monoolein). However, as opposed to phospholipids,<sup>12</sup> the interactions between monoglyceride and protein in the mixed monolayer are quite weak.

(v) Finally, at surface pressures lower than the equilibrium spreading pressure of the protein, as monoglyceride and protein coexist at the interface or at surface pressures higher than the equilibrium spreading pressure of the protein, as monoglyceride

predominates at the interface, the surface dilatational modulus is higher for  $\beta$ -casein<sup>1</sup> than for  $\beta$ -lactoglobulin mixed films (Figures 9 and 10), which confirms that the penetration in a monoglyceride monolayer is easier for  $\beta$ -casein than for  $\beta$ -lactoglobulin.

**Acknowledgment.** This research was supported by CICYT through Grant AGL2004-1306/ALI.

## References and Notes

- (1) Carrera, C.; Cejudo, M.; Rodríguez Niño, M. R.; Rodríguez Patino, J. M. *Langmuir* **2006**, *22*, 4215–4224.
- (2) Dickinson, E. *An Introduction to Food Colloids*; Oxford University Press: Oxford, U.K., 1992.
- (3) McClements, D. J. *Food Emulsions: Principles, Practice and Techniques*; 2nd ed.; CRC Press: Boca Raton, FL, 2005.
- (4) Rodríguez Niño, M. R.; Rodríguez Patino, J. M.; Carrera, C.; Cejudo, M.; García, J. M. *Chem. Eng. Commun.* **2003**, *190*, 15–47.
- (5) Horne, D.; Rodríguez Patino, J. M. In *Biopolymers at Interfaces*, 2nd ed.; Malmsten, M., Ed.; Marcel Dekker: New York, 2003; pp 857–900.
- (6) Rodríguez Patino, J. M.; Rodríguez Niño, M. R.; Carrera, C. *Curr. Opin. Colloid Interface Sci.* **2003**, *8*, 387–395.
- (7) Cejudo, M.; Carrera, C.; Rodríguez Niño, M. R.; Rodríguez Patino, J. M. *Food Hydrocolloids* **2006** (doi:10.1016/j.foodhyd.2006.08.016).
- (8) Bos, M.; Nylander, T.; Arnebrant, T.; Clark, D. C. In *Food Emulsions and their Applications*; Hasenhuette, G. L., Hartel R. W., Eds.; Chapman and Hall: New York, 1997; pp 95–146.
- (9) Wilde, P. J. *Curr. Opin. Colloid Interface Sci.* **2000**, *5*, 176–181.
- (10) Dickinson, E. *Colloids Surf., B* **2001**, *20*, 197–210.
- (11) Li, J. B.; Krägel, J.; Makievski, A. V.; Fainermann, V. B.; Miller, R.; Möhwald, H. *Colloids Surf., A* **1998**, *142*, 355–360.
- (12) Li, J. B.; Zhao, J.; Miller, R. *Nahrung* **1998**, *42*, 234–235.
- (13) Rodríguez Patino, J. M.; Carrera, C.; Rodríguez Niño, M. R. *Langmuir* **1999**, *15*, 2484–2492.
- (14) Rodríguez Patino, J. M.; Carrera, C.; Rodríguez Niño, M. R. *Food Hydrocolloids* **1999**, *13*, 401–408.
- (15) Rodríguez Niño, M. R.; Carrera, C.; Cejudo, M.; Rodríguez Patino, J. M. *J. Am. Oil Chem. Soc.* **2001**, *78*, 873–879.
- (16) Rodríguez Patino, J. M.; Carrera, C.; Rodríguez Niño, M. R.; Cejudo, M. *Langmuir* **2001**, *17*, 4003–4013.
- (17) Rodríguez Patino, J. M.; Rodríguez Niño, M. R.; Carrera, C.; Cejudo, M. *Langmuir* **2001**, *17*, 7545–7553.
- (18) Lucassen, J.; van den Tempel, M. *Chem. Eng. Sci.* **1972**, *27*, 1283–1291.
- (19) Carrera, C.; Rodríguez Niño, M. R.; Rodríguez Patino, J. M. *Colloids Surf., B* **1999**, *12*, 175–192.
- (20) Carrera, C.; Rodríguez Patino, J. M. *Langmuir* **2004**, *20*, 4530–4539.
- (21) Rodríguez Patino, J. M.; Cejudo, M. *Langmuir* **2004**, *20*, 4515–4522.
- (22) Rodríguez Patino, J. M.; Cejudo, M.; Carrera, C.; Rodríguez Niño, M. R. *Ind. Eng. Chem. Res.* **2006**, *45*, 1886–1895.
- (23) Graham, D. E.; Phillips, M. C. *J. Colloid Interface Sci.* **1979**, *70*, 427–439.
- (24) Zhao, J.; Vollhardt, D.; Brezesinski, G.; Siegel, S.; Wu, J.; Li, J. B.; Miller, R. *Colloids Surf., A* **2000**, *171*, 175–184.
- (25) Vollhardt, D.; Fainermann, V. B. *Adv. Colloid Interface Sci.* **2000**, *86*, 103–151.
- (26) Wang, X.; Zhang, Y.; Wu, J.; Wang, M.; Cui, G.; Li, J.; Brezesinski, G. *Colloids Surf., B* **2002**, *23*, 339–347.
- (27) Rodríguez Patino, J. M.; Carrera, C.; Rodríguez Niño, M. R.; Cejudo, M. *J. Colloid Interface Sci.* **2001**, *242*, 141–151.
- (28) Rodríguez Patino, J. M.; Rodríguez Niño, M. R.; Carrera, C. *J. Agric. Food Chem.* **2003**, *51*, 112–119.
- (29) Lucero, A.; Rodríguez Niño, M. R.; Carrera, C.; Rodríguez Patino, J. M.; Gunning, A. P.; Mackie, A. R. In *Food Colloids: Interactions, Microstructure and Processing*; Dickinson, E., Ed.; Royal Society of Chemistry: Cambridge, 2005; pp 160–175.